

# Studies on the Nickel Matte

## I. Nickel-Iron-Sulphur System

By

Kiyokado NISHIHARA\* and Yoshio KONDO\*

(Received January 5, 1961)

Main raw material for metallic nickel in Japan is garniellite, and the matte-smelting process is usually adopted here. The nickel matte produced in this process is, therefore, a ternary mixture of nickel, iron and sulphur, and it is usually ferromagnetic. The relationship of the magnetic properties of the nickel matte to its composition is considered to be important both from fundamental and practical points of view. The authors conducted measurements of the intensity of magnetization, thermomagnetic analyses and X-ray studies on prepared specimens of the binary system Ni-S and of the ternary system Ni-Fe-S.

In the system Ni-S and Ni-Fe-S, ferromagnetism was found in a limited region, and it is due to the metallic nickel phase in Ni-S and the nickel-iron alloy phase in Ni-Fe-S. The hexagonal phase NiS and the cubic ternary compound  $(\text{Ni, Fe})_9\text{S}_8$  were investigated with X-ray, and their lattice parameters were determined. Furthermore, the range in which  $(\text{Ni, Fe})_9\text{S}_8$  exists was also fixed. They are as follows:

$a=3.436 \text{ kX}$ ,  $c=5.351 \text{ kX}$  and  $c/a=1.557$  in NiS, and the range of the existence of  $(\text{Ni, Fe})_9\text{S}_8$ ; 22.2 atom.% Ni and 30.7 atom.% Ni in the section of 47.1 atom.% S, and

$a=10.129 \text{ kX}$  in  $(\text{Ni, Fe})_9\text{S}_8$  saturated with FeS  
 $a=10.095 \text{ kX}$  in  $(\text{Ni, Fe})_9\text{S}_8$  saturated with  $\text{Ni}_3\text{S}_2$ .

The continuous solid solution of NiS and  $\text{FeS}_{1+x}$ , the hexagonal phase  $\eta$ , was also investigated with X-ray.

The Curie temperature of the specimens in the ternary system showed rather peculiar behaviors in relation to their compositions. This peculiarity of the Curie temperature seems to be due to the deviation in the content of nickel in the alloy phase of matte. Other two magnetic transformations were also observed; one was found with the specimens in the region  $\gamma+\delta+\pi$  (see Figs. 1 and 9) at about 480°C in heating and at about 420°C in cooling. The authors considered this transformation to be related to the order-disorder transformation in the  $\text{Ni}_3\text{Fe}$  lattice. The other was found in the region  $\gamma+\varepsilon$  and in the iron side of the region  $\gamma+\varepsilon+\pi$ . This transformation was found to be due to the  $\alpha \rightleftharpoons \gamma$  transformation in the nickel-iron alloy phase.

The properties of the nickel matte taken from the converter of a nickel smelter were also examined, and the results were in good agreement with those of the prepared specimens.

---

\* Department of Metallurgy

## 1. Introduction

The usual way for manufacture of metallic nickel from garniellite in Japan is the matte-smelting process. Garniellite from New Caledonia is charged with coke breeze, gypsum and fluxes into the shaft furnace or into the open type electric furnace. Blast furnace matte containing nickel, iron and sulphur is bessemerized in the converter. The greater part of the iron is removed in this process and the converter matte consists mainly of nickel and sulphur. This converter matte is treated in one of the following two ways; (i) the matte is cast into the anode and electrolyzed, or (ii) the matte is roasted to nickel oxide and reduced with a reducing gas. Metallic nickel powder thus obtained is melted in the electric furnace and cast into the metallic nickel anode. The metallic nickel anode is refined by the Hybinette process of electrolysis.

Nickel matte, the intermediate product of this smelting process, is thus a ternary mixture of nickel, iron and sulphur, and is considered to consist of  $\text{Ni}_3\text{S}_2$ ,  $\text{FeS}$ ,  $(\text{Ni, Fe})_9\text{S}_8$  and metallic nickel or nickel-iron alloy. However, the relation between the composition of the matte and the nature of its equilibrium phases has not been settled completely by studies made heretofore<sup>1-6)</sup>.

The usual nickel matte is ferromagnetic, and its magnetic properties, such as the intensity of magnetization and the magnetic transformation temperature, are very sensitive to the composition. The nickel matte can be recovered by the magnetic separation from the nickel slag from the converter or from fused phosphorus fertilizer as practised in Japan. As will be shown later, at the final stage of the bessemerizing of the nickel matte, the Curie temperature of the matte falls rapidly, and therefore, its end point might possibly be judged by this thermomagnetic property of the matte.

The magnetic properties of the nickel matte in connection with its composition are therefore considered to be important from both fundamental and practical points of view. In this study, the authors conducted measurements of the intensity of magnetization, thermomagnetic analyses and X-ray studies mainly with prepared specimens of the nickel matte, and investigated the magnetic properties and the equilibrium components of nickel mattes at various compositions.

The results of previous studies on nickel matte containing iron may be summarized as follows:

K. Bornemann<sup>1)</sup> (1908) performed the thermal analysis of the pseudo-binary system of  $\text{Ni}_3\text{S}_2$ - $\text{FeS}$ , and found the doubtful ternary compound,  $(\text{FeS})_2\text{Ni}_3\text{S}_2$ .

R. Vogel and W. Tonn<sup>2)</sup> (1930) studied the pseudo-quarternary region Ni-Fe-FeS- $\text{Ni}_3\text{S}_2$  of the ternary system Ni-Fe-S. They conducted thermal analyses and

microscopic examinations of the specimens, and determined the equilibrium state diagram. They also stated that the ternary compound  $(\text{FeS})_2\text{Ni}_3\text{S}_2$  is present in the system. Magnetic transformation temperatures were also measured with the several specimens.

G. A. Harcourt<sup>3)</sup> (1942) found the pentlandite,  $(\text{Ni, Fe})_9\text{S}_8$  in the ternary system Ni-Fe-S.

Recently, D. Lundqvist<sup>4,5)</sup> (1947) studied on the binary system Ni-S and on the ternary system Ni-Fe-S by the method of X-ray powder photogram. He confirmed the presence of  $\text{Ni}_3\text{S}_2$  (phase  $\delta$ , rhombohedral),  $\text{Ni}_6\text{S}_5$  (phase  $\sigma$ , orthorhombic),  $\text{Ni}_7\text{S}_6$  (phase  $\varphi$ , crystalline form undetermined) and NiS (phase  $\eta$ , hexagonal) in the region between nickel and NiS of the binary system Ni-S, and the presence of  $(\text{Ni, Fe})_9\text{S}_8$  (phase  $\pi$ , cubic) in the ternary system Ni-Fe-S. He also measured the lattice parameters of these compounds, and, from these results, he presented the isothermal equilibrium sections of the system Ni-Fe-S at 200°C and 680°C. Marked differences were not found between these two sections in the region surrounded by the line Ni-Ni<sub>3</sub>S<sub>2</sub>-(Ni, Fe)<sub>9</sub>S<sub>8</sub>-FeS-Fe. The isothermal equilibrium section at 680°C presented by him is shown in Fig. 1.

Y. Itaya, H. Shimada and J. Ando<sup>6)</sup> (1953) studied the composition of nickel matte with X-ray, and confirmed the presence of  $(\text{Ni, Fe})_9\text{S}_8$ .

As stated above, ordinary nickel mattes contain nickel-iron alloy, and the

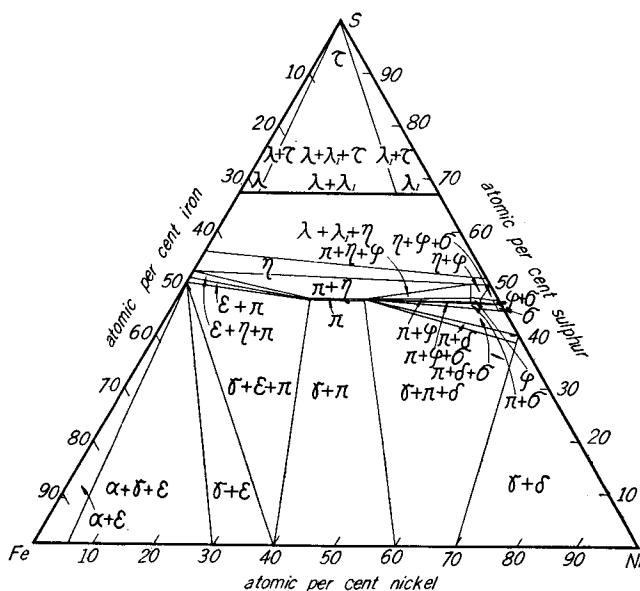


Fig. 1. Isothermal Section of System Ni-Fe-S at 680°C (by D. Lundqvist<sup>5)</sup>).

magnetic properties of the matte are influenced markedly by its constituent alloys. The particular magnetic properties of nickel-iron alloy are well-known, and detailed studies were performed on the  $\alpha \rightleftharpoons \gamma$  transformation by M. Peschard<sup>7-9</sup>), A. T. Pickles and W. Sucksmith<sup>10</sup>), K. Hoselitz and W. Sucksmith<sup>11</sup>) and by many other workers; on the other hand, O. Dahl<sup>12</sup>), O. Dahl and J. Pfaffenberger<sup>13</sup>), S. Kaya<sup>14</sup>), E. Josso<sup>15</sup>), J. Wakelin and E. L. Yates<sup>16</sup>), W. Sucksmith<sup>17</sup>), and others have studied, from various points of view, the order-disorder transformation of the Ni<sub>3</sub>Fe lattice. However, studies on the magnetic properties of nickel matte could only be found in the studies of R. Vogel and W. Tonn<sup>2</sup>).

## 2. Experimental

### 2.1. Materials

The specimens in this study were prepared by vacuum fusion in sealed quartz tube; electrolytic nickel from the Sumitomo Metal Mining Co. (>99.9%), electrolytic iron from the Showa Denko Co. (>99.9%) and redistilled sulphur were used as the starting materials. Nickel and iron chips prepared with a lathe were preheated in a vacuo of  $10^{-4}$  mm Hg at 800°C for 2 hours in order to remove the volatile impurities. The nickel and iron chips and sulphur powder were weighed and mixed, and a mixture whose total weight was about 3 g was sealed in a evacuated quartz tube (inner diameter 8 mm). The quartz tube containing the mixture was hung in a vertical electric furnace and heated up to 900°C at a heatingrate of 100°C/hr. It was kept at this temperature for 24 hours and then cooled. The product was taken out from the quartz tube, crushed and again sealed in an evacuated quartz tube. It was heated to 1100°C at a heating rate of 300°C/hr., and kept at that temperature for 5 hours to assure homogenization; it was cooled in the furnace to 600°C, kept at this temperature for 15 hours, and then quenched.

Table 1. Composition of Specimens (System Ni-S)

Specimen No.	Wt. % Ni	Wt. % S	Corresponding Compound
1	85.00	15.00	
2	80.00	20.00	
3	75.00	25.00	
4	73.30	26.70	Ni <sub>3</sub> S <sub>2</sub>
5	70.00	30.00	
6	68.71	31.29	Ni <sub>6</sub> S <sub>5</sub>
7	68.10	31.90	Ni <sub>7</sub> S <sub>6</sub>
8	65.00	35.00	
9	64.67	35.33	NiS

Table 2. Composition of Specimens (system Ni-Fe-S)

Specimen No.	Atom. % Ni	Atom. % Fe	Atom. % S	Specimen No.	Atom. % Ni	Atom. % Fe	Atom. % S
67.5·02.5·30	67.5	2.5	30	45·12·42	45	12.5	42.5
65·05·30	65	5	30	40·17·42	40	17.5	42.5
60·10·30	60	10	30	35·22·42	35	22.5	42.5
50·20·30	50	20	30	50·05·45	50	5	45
40·30·30	40	30	30	45·10·45	45	10	45
30·40·30	30	40	30	40·15·45	40	15	45
20·50·30	20	50	30	35·20·45	35	20	45
15·55·30	15	55	30	30·25·45	30	25	45
62.5·02.5·35	62.5	2.5	35	25·30·45	25	30	45
60·05·35	60	5	35	20·35·45	20	35	45
55·10·35	55	10	35	10·45·45	10	45	45
50·15·35	50	15	35	05·50·45	5	50	45
45·20·35	45	20	35	50·02·47	50	2.5	47.5
40·25·35	40	25	35	45·07·47	45	7.5	47.5
35·30·35	35	30	35	40·12·47	40	12.5	47.5
30·35·35	30	35	35	35·17·47	35	17.5	47.5
25·40·35	25	40	35	40·10·50	40	10	50
20·45·35	20	45	35	30·20·50	30	20	50
15·50·35	15	50	35	20·30·50	20	30	50
10·55·35	10	55	35	10·40·50	10	40	50
55·05·40	55	5	40				
50·10·40	50	10	40	PDNi-1	32.8	20.1	47.1
45·15·40	45	15	40	PDNi-2	31.8	21.1	47.1
40·20·40	40	20	40	PDNi-2	30.7	22.2	47.1
35·25·40	35	25	40	PD	26.5	26.5	47.1
30·30·40	30	30	40	PDFe-1	22.2	30.7	47.1
25·35·40	25	35	40	PDFe-2	21.1	31.8	47.1
20·40·40	20	40	40	PDFe-3	20.1	32.8	47.1
15·45·40	15	45	40	PDFe-4	19.1	33.8	47.1
10·50·40	10	50	40	PDFe-5	17.6	35.3	47.1
05·55·40	5	55	40				
50·07·42	50	7.5	42.5				

In this preparation procedure, the losses due to oxidation or volatilization were barely evident, and homogeneous specimens could be prepared. Nine specimens of the binary system Ni-S and sixty two specimens of the ternary system Ni-Fe-S were thus prepared, their compositions being tabulated in Tables 1 and 2.

In addition, the authors studied the nickel matte received from the Shisakajima Smelter of the Sumitomo Metal Mining Co. The assay of the nickel matte received is shown in Table 3.

Table 3. Composition of Nickel Matte (Shisakajima Smelter)

Specimen	Wt.% Ni	Wt.% Fe	Wt.% S	Wt.% Co
Blast Furnace Matte	22.74	53.08	19.17	1.36
Matte at the First Deslagging Period	37.25	28.93	26.66	1.85
Matte at the Second Deslagging Period	68.43	4.01	22.92	1.54
Converter Matte	79.25	0.22	18.60	0.88

Compositions of the specimens of Tables 1 and 2 were plotted on the ternary diagram Ni-Fe-S of Fig. 2. The compositions of the nickel matte from Shisakajima Smelter (Table 3) were also plotted on this figure. According to Fig. 2 and Table 3, the content of sulphur in the matte increases in the course of bessemerizing but decreases in the final stage.

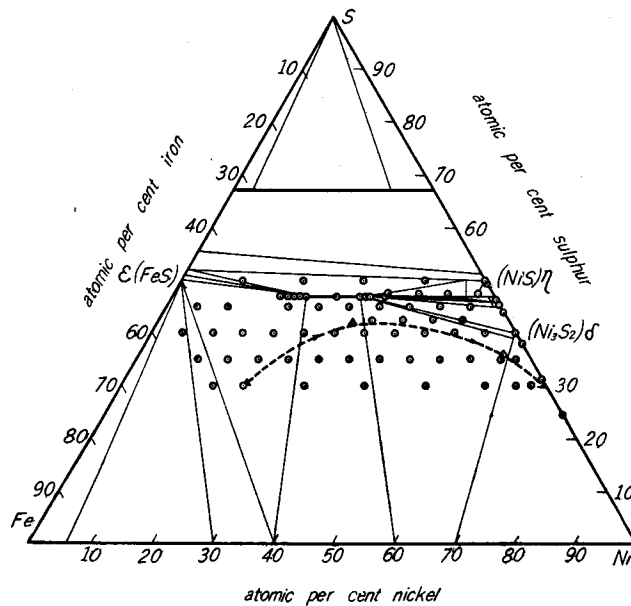


Fig. 2. Composition of the Specimens.

For convenience, the specimens of the ternary system were generally denoted with six numbers, the first two numbers showing the atomic percentage of nickel, the middle two that of iron and the last two that of sulphur. Thus the specimen whose composition is 65 atom.% Ni, 5 atom.% Fe and 30 atom.% S is designated as 65·05·30.

## 2.2. Methods of Measurement

The authors performed, in this study, measurements of the intensity of magnetization, thermomagnetic analyses and X-ray studies. Details of these methods were previously described in this Memoir<sup>18,19)</sup>, and will be omitted here. In the measurements for the thermomagnetic analyses, the specimen was sealed in an evacuated quartz tube (inner diameter 2 mm).

## 2.3. Results

### 2.3.1. Binary System Ni-S

The magnetic region in this binary system was found in the range between Ni and Ni<sub>3</sub>S<sub>2</sub>, and the specimens of higher sulphur content than Ni<sub>3</sub>S<sub>2</sub> were non-magnetic. The relative intensity of magnetization of the specimens in this magnetic region was measured, and they are plotted against the content of Ni<sub>3</sub>S<sub>2</sub> in Fig. 3. The intensity of magnetization of the specimen decreases

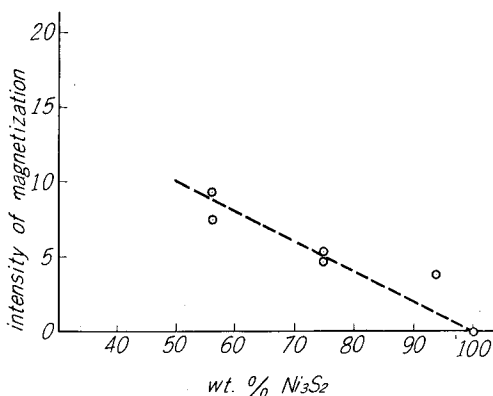


Fig. 3. Relative Intensity of Magnetization (Binary System Ni-S).

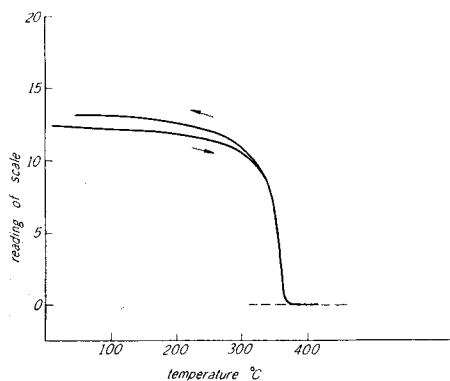


Fig. 4. The Thermomagnetic Analysis of the Specimen 80 wt.% Ni and 20 wt.% S.

linearly when the content of Ni<sub>3</sub>S<sub>2</sub> increases. Similar curves of the thermomagnetic analysis were obtained with the ferromagnetic specimens in that region. The Curie temperature was found at about 355°C for each specimen. As an example of such a curve, the result for the specimen of 80 wt.% Ni and 20 wt.% S are shown in Fig. 4. From the results above-mentioned, it was concluded that the ferromagnetism in the binary system Ni-S is due to the metallic nickel contained in the specimens.

X-ray powder photograms were taken with the specimens in this system. As mentioned previously, in the region of the composition between Ni and NiS, the following four compounds have been reported to be present<sup>4)</sup>; Ni<sub>3</sub>S<sub>2</sub>, Ni<sub>6</sub>S<sub>5</sub>, Ni<sub>7</sub>S<sub>6</sub> and NiS. Diffraction patterns obtained with the specimens whose com-

positions correspond to these compounds are shown in Fig. 5. The lattice parameters and the axial ratio of the hexagonal NiS were calculated from the diffraction pattern by the least square method of Cohen<sup>22</sup>. These values were

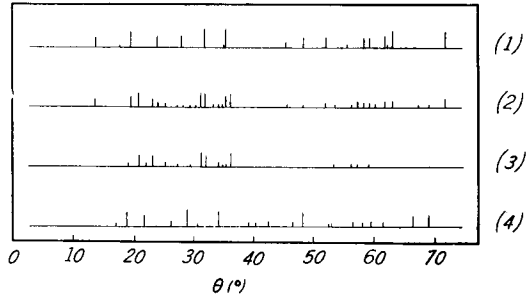
$$a = 3.436 \text{ kX}, \quad c = 5.351 \text{ kX} \quad \text{and} \\ c/a = 1.557.$$

They are in good agreement with those obtained by D. Lundqvist<sup>4</sup>.

In Fig. 5, the diffraction pattern of the specimen whose composition corresponds to Ni<sub>6</sub>S<sub>5</sub> seems to be that of a mixture of Ni<sub>3</sub>S<sub>2</sub> and Ni<sub>7</sub>S<sub>6</sub>. It may be due to the instability of Ni<sub>6</sub>S<sub>5</sub> at the quenching temperature of 600°C used in this study. Ni<sub>6</sub>S<sub>5</sub> is said to be stable only between 400°C and 560°C<sup>21</sup>.

**2.3.2. Ternary System Ni-Fe-S**

The magnetic region in the ternary system was found to lie within the composition range enclosed by the line Ni-Ni<sub>3</sub>S<sub>2</sub>-(Ni, Fe)<sub>9</sub>S<sub>8</sub>-FeS-Fe in Fig. 1. Specimens outside of this area were non-magnetic. The relative intensity of magnetization of the magnetic specimens was measured. Fig. 6 shows contour



(1) Ni<sub>3</sub>S<sub>2</sub> (2) Ni<sub>6</sub>S<sub>5</sub> (3) Ni<sub>7</sub>S<sub>6</sub> (4) NiS  
Fig. 5. Representative Diffraction Pattern in the System Ni-S.

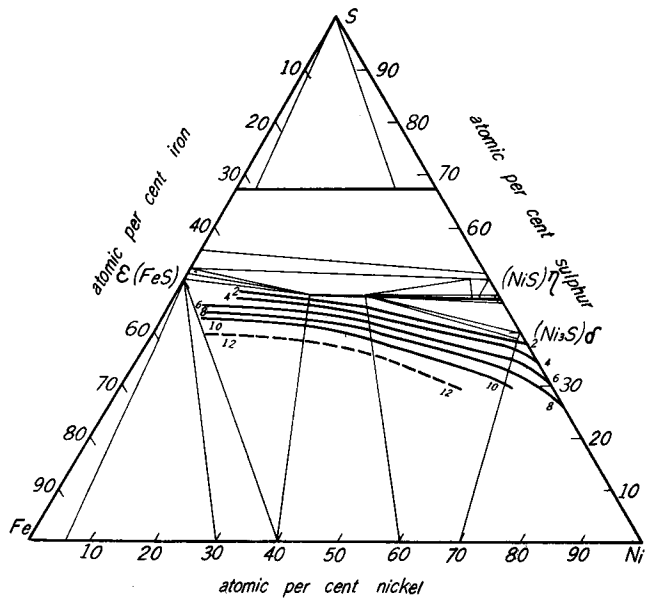


Fig. 6. The Contour of the Relative Intensity of Magnetization (Ternary System Ni-Fe-S).



lines for the relative intensity of magnetization. For the strong magnetic specimens whose relative intensity of magnetization ( $I/w$ )<sup>19)</sup> was higher than 10, the precision of the measurement was poor, and therefore, the contour line is shown as a broken line. As shown in the figure, the intensity of magnetization decreases toward the line  $\text{Ni}_3\text{S}_2$ - $(\text{Ni, Fe})_9\text{S}_8$ -FeS in Fig. 1, and it is considered that the ferromagnetism in this ternary system is due to the nickel-iron alloy contained in the specimen and that the compounds such as  $\text{Ni}_3\text{S}_2$ ,  $(\text{Ni, Fe})_9\text{S}_8$  and FeS are not ferromagnetic.

The thermomagnetic analyses were performed with ferromagnetic specimens of the ternary system. Various curves of the thermomagnetic analysis were obtained according to compositions of the specimen, and the authors classified these curves into the following nine groups (A) to (I). Representative curves of the thermomagnetic analysis for each group are shown in Fig. 7.

(A): Hysteresis in the curve of the thermomagnetic analysis was practically absent, and the Curie temperatures were found to lie in the range of temperature between 450°C and 500°C. This type of curve was found in specimens whose iron content is low and whose composition lies near the bordering system of Ni-S (region  $\gamma+\delta$ ). (Specimens 67.5·02.5·30 and 62.5·02.5·35)

(B): The intensity of magnetization decreases continuously in heating, and the Curie temperature is found at about 500°C. On the other hand, in cooling, a knick point is observed between 400° and 420°C. This type of curve was observed with specimens of high nickel content in the region  $\gamma+\delta$  or in its neighbourhood. (Specimens 65·05·30 and 60·05·35)

(C): In the heating curve of the analysis, a knick point occurs at about 480°C, and the Curie temperature appears at about 600°C. In the cooling curve, the knick point is observed at 400°C to 420°C. The specimens in the region  $\gamma+\delta+\pi$  of 30 and 35 atom. % sulphur belong to this type. (Specimens 60·10·30, 50·20·30, 55·10·35 and 45·20·35)

(D): The shape of the curve is almost similar to the type (C). The difference between them is that hysteresis is observed below 500°C in type (D). The specimens in the region  $\gamma+\delta+\pi$  of higher sulphur content belong to this type. (Specimens 45·15·40, 40·20·40, 35·25·40, 40·17·42 and 35·22·42)

(E): In heating, the intensity of magnetization decreases rapidly to about 480°C, and above this temperature, the intensity of magnetization shows a very low value. In cooling, at the temperature of 440°C to 450°C, the intensity increases very rapidly. This type of curve was observed with specimens near the line of  $\text{Ni}_3\text{S}_2$ - $(\text{Ni, Fe})_9\text{S}_8$  in the region  $\gamma+\delta+\pi$ . (Specimens 55·05·40, 50·10·40, 35·12·47 and 35·20·45)

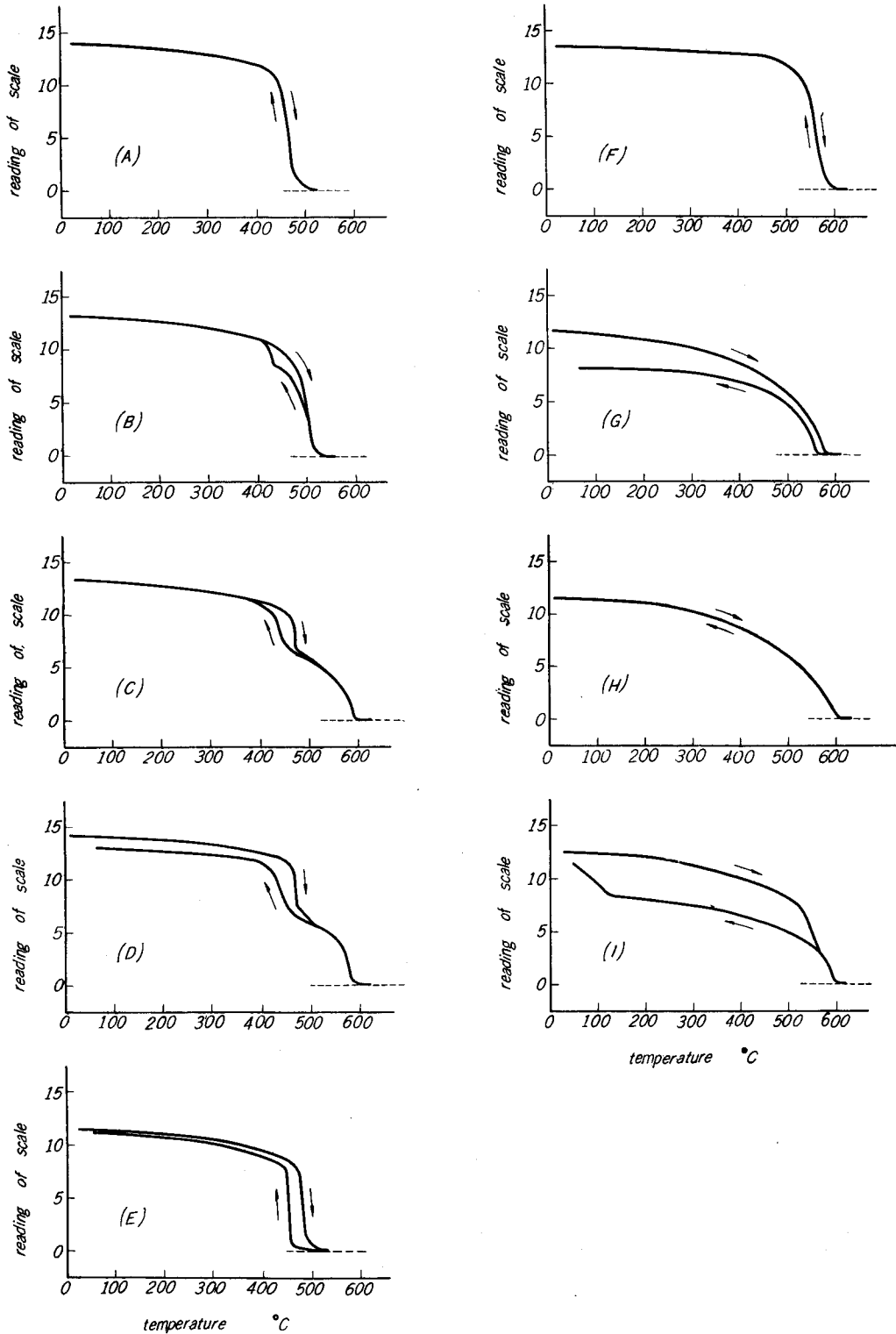


Fig. 7. The Curves of Thermomagnetic Analysis in the Ternary System Ni-Fe-S.

(F): The curve of the thermomagnetic analysis shows no hysteresis, and the Curie temperature is found at about 600°C. The specimens in the region  $\gamma+\pi$  of 30, 35 and 40 atom. % sulphur show this type of the curve. (Specimens 40·30·30, 40·25·35, 35·30·35, 30·35·35, 25·40·35, 30·30·40 and 25·35·40)

(G): This type of the curve shows the Curie temperature at about 600°C, and hysteresis between heating and cooling was also observed. This type of curve was observed with the specimens in the region  $\gamma+\pi$  and  $\gamma+\varepsilon+\pi$  near the phase  $(\text{Ni, Fe})_3\text{S}_8$ . (Specimens 30·25·45 and 20·35·45)

(H): Hysteresis between heating and cooling was observed, and the Curie temperature was found at about 600°C. In heating, the intensity of magnetization decreases at a comparatively constant rate, a feature which distinguishes it from (F). The specimens in the region  $\gamma+\varepsilon+\pi$  belong to this type. (Specimens 30·40·30, 20·50·30, 20·45·35, 20·40·40, 15·45·40, 10·45·45 and 05·50·45)

(I): In heating, the intensity of magnetization decreases continuously, and the Curie temperature is found at about 570°C. On the other hand, in the cooling curve, the intensity of magnetization shows a much lower value, but at about 100°C, the intensity increases rapidly and reaches the original value; thus a hysteresis between heating and cooling was observed. This type of curve was observed in the region  $\gamma+\varepsilon$  and in the lower nickel content part of the region  $\gamma+\varepsilon+\pi$ . (Specimens 15·55·30, 15·50·35, 10·55·35, 10·50·40 and 05·55·40)

The magnetic transformation temperatures observed in these measurements are plotted in Fig. 8 against the atomic percentage of nickel for each section of constant sulphur content. In this figure, the Curie temperature rises with decreasing content of nickel and reaches about 600°C for each section. It descends a little from 600°C as the content of nickel falls below about 20 atom. %. The magnetic transformation, observed

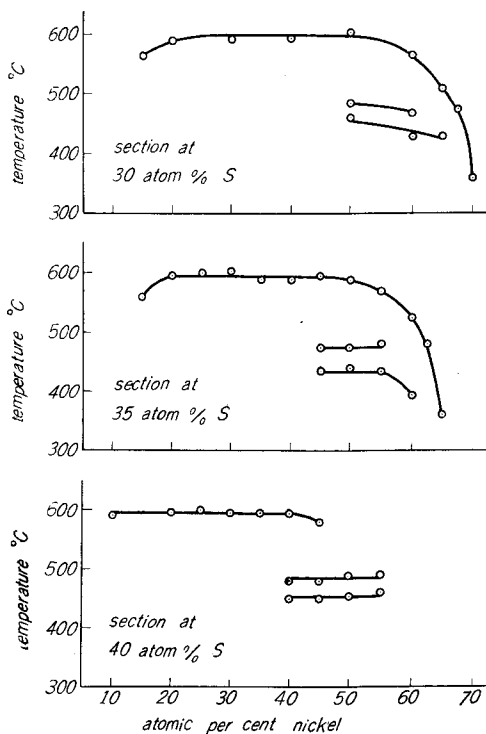


Fig. 8. Magnetic Transformation Temperature in the Ternary System Ni-Fe-S.

at about 480°C in heating and at about 450°C in cooling, becomes sharper with increasing the sulphur content. In the section of 30 atom. % sulphur, its temperature rises a little with decreasing nickel content, but changes in the temperature were barely observable in the sections of higher sulphur content. This magnetic transformation temperature, which was observed as a hysteresis between heating and cooling in the thermomagnetic analysis was found in the specimens of the type (B), (C), (D) and (E) above mentioned. Most of the composition of these specimens belongs to the region  $\gamma + \delta + \pi$  in Fig. 1. Another large hysteresis between the heating curve and the cooling curve was observed in the specimens in the iron side of the region  $\gamma + \epsilon + \pi$  and in the region  $\gamma + \epsilon$  (type (I)).

X-ray powder photographs of the specimens of the ternary system were examined and the phases identified in the specimens were summarized in Fig. 9.

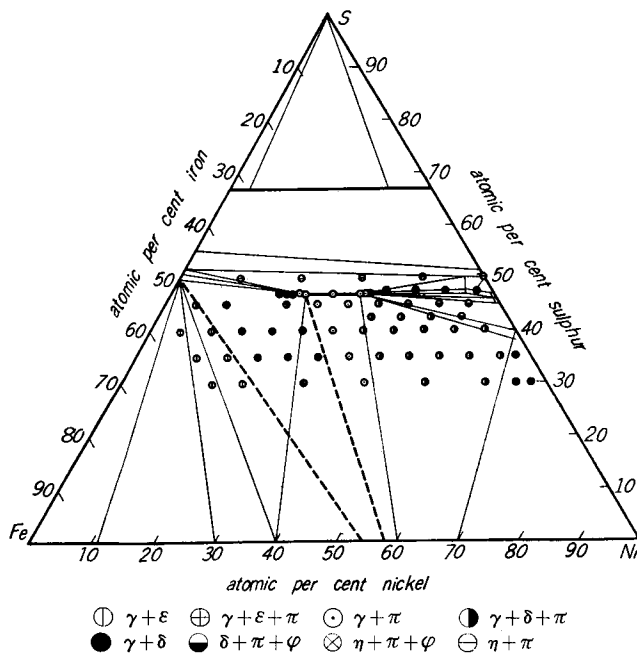


Fig. 9. Phases Identified in the Ternary System Ni-Fe-S.

Among the phases identified,  $(\text{Ni}, \text{Fe})_9\text{S}_8$  belongs to the cubic system, and its range of existence is said to extend from  $(\text{Ni}_{18}, \text{Fe}_{18})\text{S}_{32}$  to  $(\text{Ni}_{12}, \text{Fe}_{24})\text{S}_{32}$  according to G. A. Harcourt<sup>3,6)</sup>, and from  $58 \pm 2\%$  to  $42 \pm 2\%$  of Fe in the ratio  $\text{Fe}/(\text{Fe} + \text{Ni})$  according to D. Lundqvist<sup>5)</sup>. The lattice parameter,  $a$ , was reported by Harcourt<sup>3,6)</sup> as  $9.91 \text{ kX}$  in  $(\text{Ni}_{18}, \text{Fe}_{18})\text{S}_{32}$  and  $10.09 \text{ kX}$  in  $(\text{Ni}_{12}, \text{Fe}_{24})\text{S}_{32}$ .

D. Lundquist<sup>5)</sup> measured  $a$  as 10.175  $kX$  in  $(Ni, Fe)_9S_8$  saturated with FeS and 10.075  $kX$  in  $(Ni, Fe)_9S_8$  saturated with  $Ni_3S_2$ . In this study, the authors tried to determine the range of existence of the compound by measuring its lattice parameter. Several specimens whose compositions were near the phase  $(Ni, Fe)_9S_8$  were prepared, their X-ray powder photograms were taken, the indices of the diffraction planes were determined by the method of Straumanis<sup>23)</sup> and the lattice parameter was calculated by the method of Bradley and Jay<sup>24)</sup>. The lattice parameter  $a$  is plotted against the content of nickel in Fig. 10. It was found from this figure that the value of the lattice parameter varies linearly between 30.7 atom. % Ni and 22.2 atom. % Ni and it shows an almost fixed value below 22.2 atom. % Ni or above 30.7 atom. % Ni. From this result of the measurement, the authors determined the range of the existence of the phase  $(Ni, Fe)_9S_8$  between 22.2 atom. % Ni and 30.7 atom. % Ni. The lattice parameter  $a$  were

$$a = 10.129 \text{ } kX \text{ in } (Ni, Fe)_9S_8 \\ \text{saturated with FeS and}$$

$$a = 10.095 \text{ } kX \text{ in } (Ni, Fe)_9S_8 \\ \text{saturated with } Ni_3S_2.$$

They coincide fairly with the values obtained by D. Lundqvist<sup>5)</sup> which are also plotted in Fig. 10.

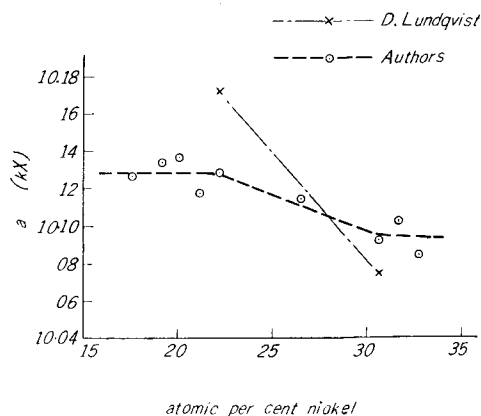


Fig. 10. The Lattice Parameter of  $(Ni, Fe)_9S_8$ .

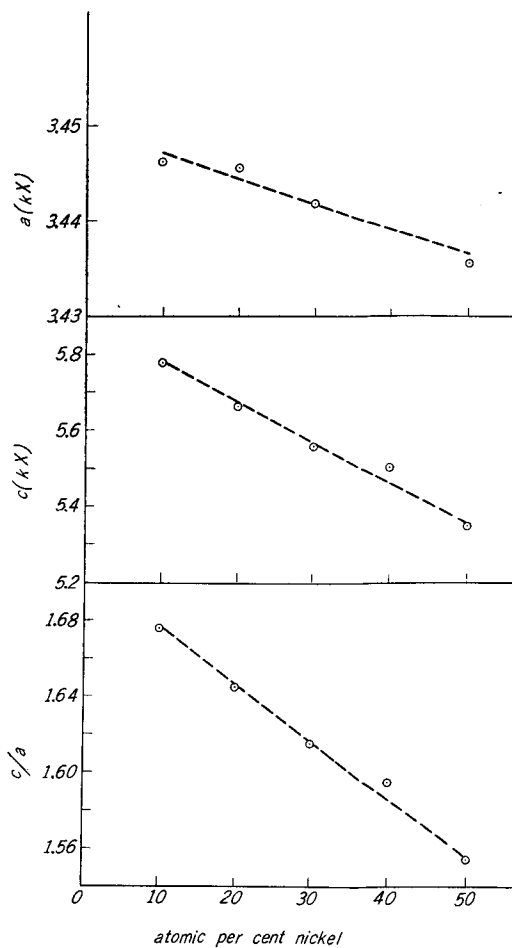


Fig. 11. The Lattice Parameters and the Axial Ratios of the Hexagonal Phase  $\eta$ .

In the isothermal equilibrium section at 680°C of D. Lundqvist<sup>5)</sup>, Fig. 1, the hexagonal phase  $\gamma$  is shown as a continuous solid solution of NiS and FeS<sub>1+x</sub>. In this study, the lattice parameters  $a$ ,  $c$  and the axial ratio  $c/a$  of the phase saturated with the phase  $\pi$  were determined by the least square method of Cohen<sup>22)</sup> with specimens of 50 atom.% S. The results are shown in Fig. 11. The lattice parameters and the axial ratio increase linearly with decreasing nickel content.

### 2.3.3. Some Studies of the Nickel Matte taken from the Nickel Converter

The specimens of the nickel matte sent from Shisakajima Smelter were investigated by means of measurements of the intensity of magnetization, thermomagnetic analysis and X-ray. The composition of the specimens are shown above in Table 3.

Values of the relative intensity of magnetization for the four specimens of nickel matte are shown in Fig. 12. It decreases in the initial stage of bessemerizing and increases in the final stage. This behavior of the intensity of magnetization can be adequately explained in terms of changes in the composition of the matte during the conversion. The intensity of magnetization of the blast furnace matte is extraordinarily high, but those of the other three specimens agree well with the values of the prepared specimen of similar composition in Fig. 6.

The results of the thermomagnetic analysis of the nickel matte are shown in Fig. 13. The curves of the thermomagnetic analysis of the blast furnace matte, the matte at the first deslagging period, the matte at the second deslagging period and the converter matte resemble the curves of types (H), (D), (C), and (A) shown in Fig. 7, respectively. This seems to be reasonable considering the composition of the mattes.

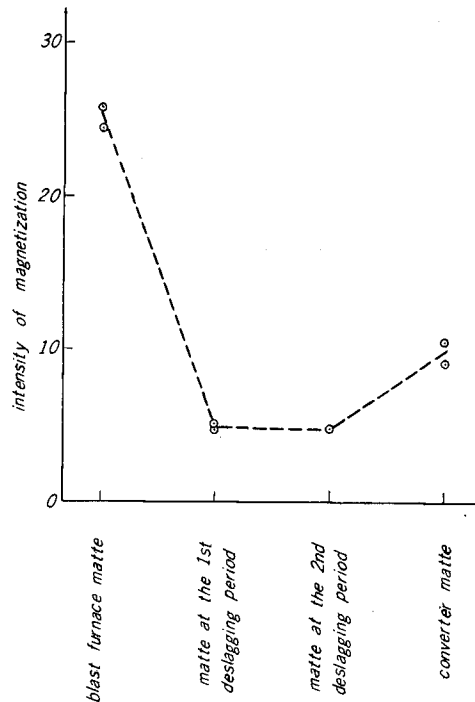


Fig. 12. The Relative Intensity of Magnetization of the Nickel Matte.

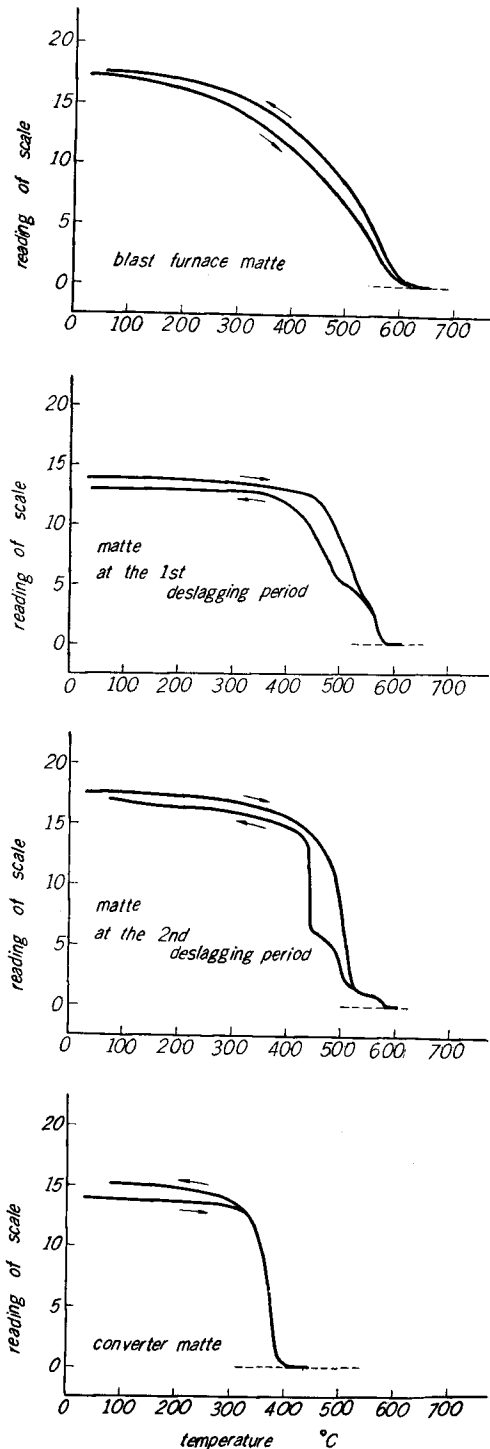


Fig. 13. The Thermomagnetic Analysis of the Nickel Matte.

The phases of the four specimens of the nickel matte identified by means of the X-ray powder photographs are summarized in Table 4. These also are in good agreement with those of the prepared specimens in Fig. 9.

Table 4. Phases Identified in the Nickel Matte

Specimen	Phases Identified
Blast Furnace Matte	$\gamma + \varepsilon + \pi$
Matte at the First Deslagging Period	$\gamma + \pi$
Matte at the Second Deslagging Period	$\gamma + \delta + \pi$
Converter Matte	$\gamma + \delta$

### 3. Discussion

The magnetic properties of the nickel-iron alloy have been investigated by many workers. According to the equilibrium phase diagram<sup>25)</sup> of Fig. 14, the Curie temperature of the alloy rises from 355°C, the Curie temperature of nickel, with decreasing nickel content. The maximum Curie temperature is 612°C at about 67 atom.% Ni. The Curie temperature decreases with further decrease in the content of nickel below 67 atom.%. In the diagram, the Curie temperature intersects the  $\alpha \rightleftharpoons \gamma$  transformation temperature at about 40 atom.% Ni. The order-disorder transformation of the Ni<sub>3</sub>Fe lattice is shown in the figure with a broken line. This transformation temperature is 503°C at 75 atom.% Ni.

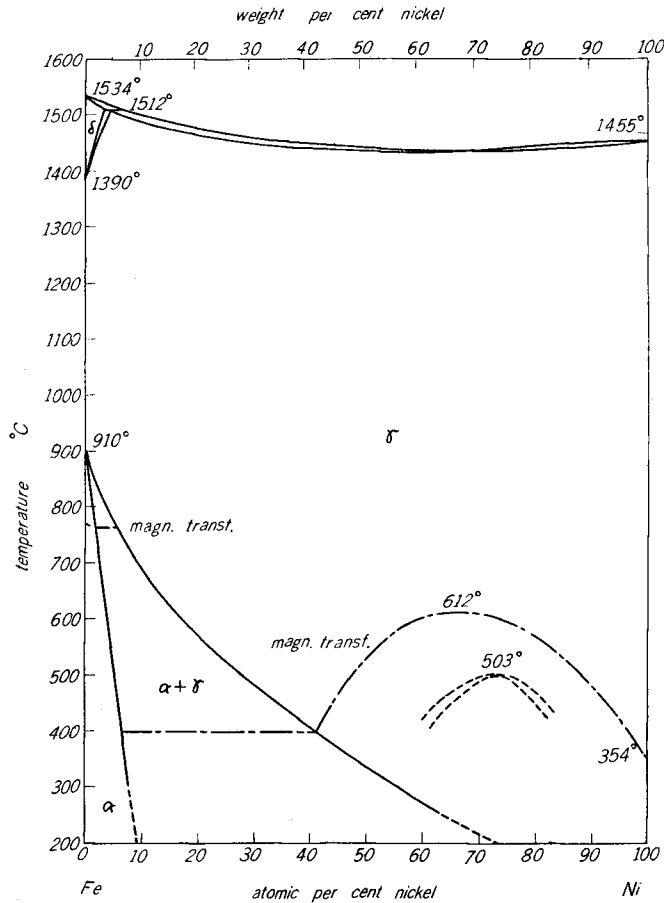


Fig. 14. The Equilibrium Phase Diagram of Nickel-Iron (M. Hansen<sup>25</sup>).

As described previously in 2.3.2., the Curie temperature of specimens of the ternary system Ni-Fe-S rises from 355°C (the Curie temperature of nickel) with decreasing nickel content, reaches a maximum at about 600°C, and then decreases a little when the content of nickel decreases below a value of about 20 atom. %.

The phases identified by X-ray in the specimens of the ternary system shown in Fig. 9 agree well with the results by D. Lundquist<sup>5)</sup> in the nickel side of the phase  $(\text{Ni, Fe})_9\text{S}_8$ , but differences were observed in the iron side of  $(\text{Ni, Fe})_9\text{S}_8$ . Namely, in the specimens of 20·50·30, 15·55·30, 15·50·35, 10·55·35, 10·50·40 and 05·50·45 which are supposed to be composed of the phase  $\gamma$ ,  $\epsilon$  and  $\pi$  according to Lundqvist, the phase  $\pi$  could not be identified in this study, and the specimens 30·40·30, 30·35·35 and 25·35·40 which are supposed to be composed of the phases



$\gamma$  and  $\pi$  according to Lundqvist were found, in this study, to be composed of the phases  $\gamma$ ,  $\epsilon$  and  $\pi$ . These results of the X-ray powder photograms suggest that the composition of the alloy phase  $\gamma$  at equilibrium in the region  $\gamma + \epsilon + \pi$  is not about 40 atom. % Ni, but 50 to 60 atom. % Ni as shown with a broken line in Fig. 9. The lattice parameter  $a$  of the phase  $(\text{Ni, Fe})_9\text{S}_8$  in the specimens below 50 atom. % sulphur are shown in Fig. 15. In this figure, the parameter was plotted against the atomic percentage of nickel for each section of the constant sulphur content. It was found, from the figure, that the lattice parameter  $a$  of the phase  $(\text{Ni, Fe})_9\text{S}_8$  present in the specimens of each section changes from the value of the phase saturated with  $\text{Ni}_3\text{S}_2$  to that saturated with  $\text{FeS}$  as the nickel content decreases. This change of the parameter occurs in a peculiar range of the content of nickel for each section. These points of change of the parameter coincide well with the above mentioned boundary line of the region  $\gamma + \pi$  and the region  $\gamma + \epsilon + \pi$  (right broken line in Fig. 9) and the boundary line of the region  $\gamma + \delta + \pi$  and the region  $\gamma + \pi$  (thin line in Fig. 9). From this result, the content of nickel in the alloy phase at equilibrium in the region  $\gamma + \epsilon + \pi$  was again confirmed.

From the above discussion, the reason for the strange behavior of the Curie temperature of specimens in the ternary system Ni-Fe-S may be explained in terms of changes in the nickel

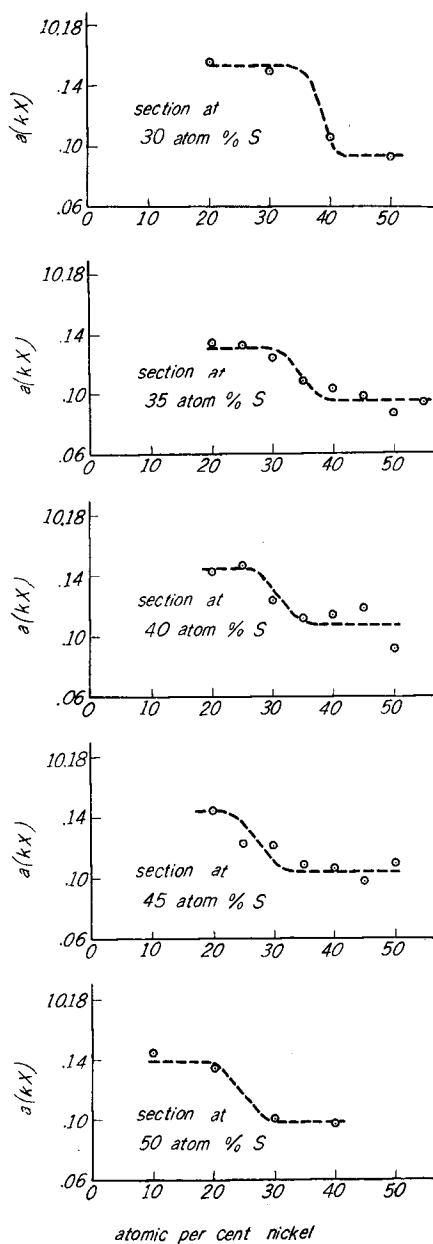


Fig. 15. The Lattice Parameter  $a$  of the Phase  $(\text{Ni, Fe})_9\text{S}_8$  present in the specimens.

content of the alloy phase as follows; in nickel matte, the content of nickel in alloy phase contained in the matte does not change widely even when the content of nickel in the matte changes considerably. The content of nickel in the alloy phase decreases below 50 atom. % when nickel content of matte becomes less than about 20 atom. %.

The magnetic transformation temperature found at about 480°C in heating and at about 450°C in cooling with the specimens of the type (B), (C), (D) and (E) in Fig. 7 which belong to the region  $\gamma + \delta + \pi$  is characteristic of the ternary system Ni-Fe-S. In the binary system Ni-Fe, this magnetic transformation temperature has not been observed in studies made heretofore<sup>7-16</sup>). In the author's opinion, this magnetic transformation temperature seems to be due to the order-disorder transformation in the Ni<sub>3</sub>Fe lattice of the alloy phase, because

- i. the transformation temperature agrees fairly well with the order-disorder transformation temperature of the Ni<sub>3</sub>Fe lattice,
- ii. the amount of change in the intensity of magnetization in this transformation is largest in the specimens whose composition is on the line combining S and Ni<sub>3</sub>Fe in the ternary diagram of Ni-Fe-S, and
- iii. no ferromagnetic compound other than the Ni-Fe alloy was observed in the ternary system Ni-Fe-S in this study.

The amount of the change of the intensity of magnetization in this transformation becomes a little larger when the specimens are heated at 430°C for long time. As examples, the curves of the thermomagnetic analysis of the specimens 60·10·30 and 45·15·40 quenched from 600°C and heated at 430°C for 1000 hours are shown in Fig. 16.

On the curve of the thermomagnetic analysis of the specimens in the region  $\gamma + \epsilon$  and in the lower nickel content part of the region  $\gamma + \epsilon + \pi$ , hysteresis between heating and cooling was observed (type (I)). The content of nickel in the alloy phase  $\gamma$  of these specimens is thought to be below 50 atom. %, as mentioned above. And in the nickel-iron alloy of such composition, the  $\alpha \rightleftharpoons \gamma$  transformation appears<sup>7-11</sup>). The  $\alpha \rightleftharpoons \gamma$  transformation temperature in the nickel-iron alloy at its equilibrium state is shown in Fig. 14, but a very long time is necessary to attain this equilibrium and in the quasi-equilibrium state, such as exists in continuous heating or cooling at a constant rate, the transformation temperatures vary widely from those shown in Fig. 14<sup>25</sup>). M. Peschard<sup>7-9</sup>), A. T. Pickles and W. Sucksmith<sup>10</sup>) have performed thermomagnetic analyses of this  $\alpha \rightleftharpoons \gamma$  transformation in the Ni-Fe alloy. They obtained curves similar to type (I) shown in Fig. 7, and hysteresis between heating and cooling was also observed. Accordingly, the magnetic transformation temperature of about 570°C in heating in type (I)

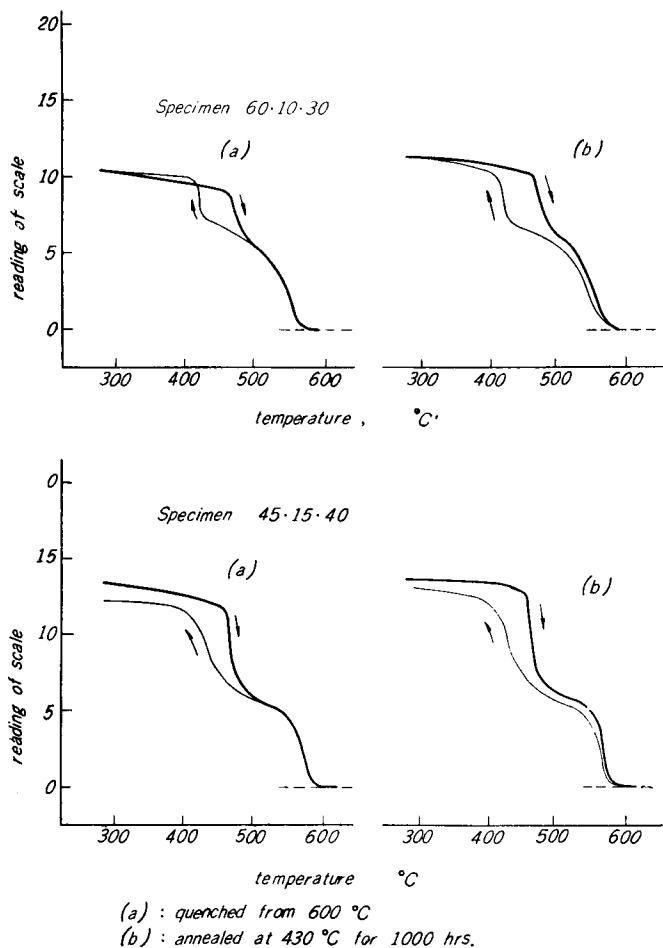


Fig. 16. The Thermomagnetic Analysis of the Specimens 60-10-30 and 45-15-40.

corresponds to the  $\alpha \rightarrow \gamma$  transformation in heating, and its transformation at about 100°C in cooling to the  $\gamma \rightarrow \alpha$  transformation.

#### 4. Summary

The authors performed measurements of the intensity of magnetization, thermomagnetic analyses and X-ray studies with specimens of the system Ni-S and Ni-Fe-S prepared from nickel, iron and sulphur and with the nickel matte received from a nickel smelter. The relation between the compositions of nickel mattes and their magnetic properties were studied and the results are summarized as follows:

1) In the binary system Ni-S, the specimens whose compositions lie in the region between Ni and  $\text{Ni}_3\text{S}_2$  show ferromagnetism. The intensity of magnetization of the specimens decreases linearly with increasing sulphur content. The Curie temperature was located at  $355^\circ\text{C}$  for all these ferromagnetic specimens. Therefore, it is concluded that the ferromagnetism in this binary system is due to the metallic nickel component. The lattice parameters and the axial ratio of the hexagonal NiS were calculated to be as follows.

$$a = 3.436 \text{ kX}, \quad c = 5.351 \text{ kX} \quad \text{and} \quad c/a = 1.557.$$

2) In the ternary system Ni-Fe-S, the ferromagnetic region was found to be enclosed within the line  $\text{Ni-Ni}_3\text{S}_2-(\text{Ni, Fe})_9\text{S}_8\text{-FeS-Fe}$  of the ternary diagram. The intensity of magnetization of the specimen decreases when the composition changes toward the line  $\text{Ni}_3\text{S}_2-(\text{Ni, Fe})_9\text{S}_8\text{-FeS}$ . The specimens whose sulphur content are higher than this line were paramagnetic. The curves of the thermomagnetic analysis of these ferromagnetic specimens in the ternary system were classified by the authors into nine groups as shown in Fig. 7. A magnetic transformation temperature was found in the specimens in the region  $\gamma + \delta + \pi$  at about  $480^\circ\text{C}$  in heating and at about  $420^\circ\text{C}$  in cooling. This magnetic transformation is thought by the authors to be due to the order-disorder transformation in the lattice  $\text{Ni}_3\text{Fe}$ . In the specimens of higher content of iron such as in the region  $\gamma + \epsilon$  and in the iron side of the region  $\gamma + \epsilon + \pi$ , another hysteresis between heating and cooling was observed. This hysteresis is due to the  $\alpha \rightleftharpoons \gamma$  transformation in the Ni-Fe alloy contained in the specimens.

The magnetic transformation temperatures measured in the thermomagnetic analyses were plotted against the content of nickel in the sections of constant sulphur content (Fig. 8). The Curie temperatures of the specimens in each section were found to increase from  $355^\circ\text{C}$ , the Curie temperature of nickel, as the nickel content decreased. It reaches at about  $600^\circ\text{C}$  and maintains this temperature over a fairly wide range of nickel content. It decreases slightly from  $600^\circ\text{C}$  when the nickel content decreases below about 20 atom. %.

The phases identified by X-ray in the ferromagnetic region of the ternary system were  $\text{Ni}_3\text{S}_2$ ,  $(\text{Ni, Fe})_9\text{S}_8$ , FeS and the Ni-Fe alloy. The range of existence of the phase  $(\text{Ni, Fe})_9\text{S}_8$  was between 22.2 atom. % Ni and 30.7 atom. % Ni in the section of 47.1 atom. % S. The lattice parameters of this cubic phase were

$$a = 10.129 \text{ kX} \text{ in } (\text{Ni, Fe})_9\text{S}_8 \text{ saturated with FeS and} \\ a = 10.095 \text{ kX} \text{ in } (\text{Ni, Fe})_9\text{S}_8 \text{ saturated with Ni}_3\text{S}_2.$$

These value were in fair agreement with those obtained by D. Lundqvist. The

lattice parameters of the phase  $(\text{Ni, Fe})_9\text{S}_8$  were also measured in the specimens whose sulphur content was 30, 35, 40, 45 and 50 atom.%. From results above-mentioned, it may be said that in the iron side of the phase  $(\text{Ni, Fe})_9\text{S}_8$ , the isothermal equilibrium section determined in this study was somewhat different from the result of Lundqvist (Fig. 1); and from this, the content of nickel in the alloy phase  $\gamma$  at equilibrium in the region  $\gamma + \epsilon + \pi$  is considered to be about 50 to 60 atom.%. The lattice parameters and the axial ratios of the continuous solid solution of the phase  $\eta$  between  $\text{NiS}$  and  $\text{FeS}_{1+x}$  were found to increase linearly with decreasing nickel content.

3) The specimens of the nickel matte received from Shisakajima Smelter of Sumitomo Metal Mining Co. were also investigated. The intensity of magnetization of the nickel matte decreases in the initial stage of the bessemerizing, and in its final stage the intensity increases. This is due to the variation of the content of sulphur in the matte. The results of the thermomagnetic analysis and the X-ray powder photograms are in good agreement with those of the ternary system Ni-Fe-S mentioned in 2).

#### Acknowledgements

The nickel mattes used in this study were sent from Shisakajima Smelter of Sumitomo Metal Mining Co. The authors express their gratitude to the research staff at the smelter.

Parts of this study were made possible by financial grants from the Ministry of Education.

#### References

- 1) K. Bornemann: *Metallurgie*, **5**, 61, (1908).
- 2) R. Vogel und W. Tonn: *Arch. für das Eisenhüttenw.*, **3**, 769, (1930).
- 3) G. A. Harcourt: *Am. Mineralogist*, **27**, 63, (1942).
- 4) D. Lundqvist: *Ark. för Kemi, Mineralogi och Geologi*, **24A**, No. 21, 1, (1947).
- 5) D. Lundqvist: *ibid.*, **24A**, No. 22, 1, (1947).
- 6) Y. Itaya, H. Shimada and J. Ando: *Journal of the Min. and Met. Inst. of Japan*, **74**, 927, (1958).
- 7) M. Peschard: *Rev. Métallurgie*, **22**, 490, (1925).
- 8) M. Peschard: *ibid.*, **22**, 581, (1925).
- 9) M. Peschard: *ibid.*, **22**, 663, (1925).
- 10) A. T. Pickles and W. Sucksmith: *Proc. Royal Soc., (London)*, **A175**, 331, (1940).
- 11) K. Hoselitz and W. Sucksmith: *ibid.*, **A181**, 303, (1943).
- 12) O. Dahl: *Z. für Metallkunde*, **24**, 107, (1932).
- 13) O. Dahl und J. Pfaffenberger: *ibid.*, **25**, 241, (1933).
- 14) S. Kaya: *J. Fac. Sci. Hokkaido Imp. Univ.*, (2), **2**, (2), 29 (1938); *Z. Metallkunde*, **31**, 212, (1939).
- 15) E. Josso: *Rev. Métallurgie*, **47**, 769, (1950).
- 16) J. Wakelin and E. L. Yates: *Proc. Phys. Soc., (London)*, **B66**, 221, (1953).

- 17) W. Sucksmith: *J. Phys. et Radium*, **12**, 430, (1951).
- 18) K. Nishihara and Y. Kondo: *This Memoir* **10**, 285, (1958).
- 19) K. Nishihara and Y. Kondo: *ibid.*, **11**, 214, (1959).
- 20) K. Bornemann: *Metallurgie*, **5**, 13 (1908); **7**, 667 (1910).
- 21) M. Hansen: *Constitution of Binary Alloys*, 1034 (McGraw Hill), (1958).
- 22) M. U. Cohen: *Rev. Sci. Instruments*, **6**, 68 (1935); **7**, 155 (1936).
- 23) M. Straumanis: *Z. Krist.*, **104**, 167 (1942); *Am. Mineralogist*, **37**, 48 (1952).
- 24) A. J. Bradley and A. H. Jay: *Proc. Phys. Soc.*, (London), **44**, 563 (1932).
- 25) M. Hansen: *Constitution of Binary Alloys*, 677 (McGraw Hill). (1958).